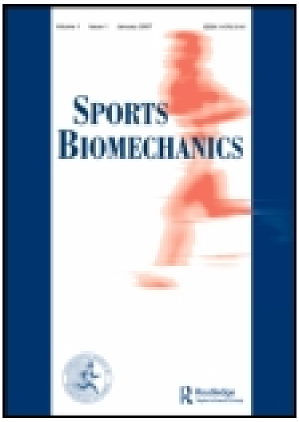

Sports Biomechanics
Publication details, including instructions for authors and subscription information:
http://www.tandfonline.com/loi/rspb20

Methodological considerations for the 3D measurement of the X-factor and lower trunk movement in golf

Christopher Joyce [a], Angus Burnett [a b] & Kevin Ball [c]

[a] School of Exercise, Biomedical and Health Sciences, Edith Cowan University, Perth, Australia

[b] Department of Sports Science and Physical Education, Chinese University of Hong Kong, Shatin, Hong Kong

[c] School of Sport and Exercise Science, Institute of Sport, Exercise and Active Living, Victoria University, Melbourne, Australia

Available online: 27 Oct 2010

To cite this article: Christopher Joyce, Angus Burnett & Kevin Ball (2010): Methodological considerations for the 3D measurement of the X-factor and lower trunk movement in golf, Sports Biomechanics, 9:3, 206-221

To link to this article: http://dx.doi.org/10.1080/14763141.2010.516446

Sports Biomechanics
September 2010; 9(3): 206–221

Routledge
Taylor & Francis Group

Methodological considerations for the 3D measurement of the X-factor and lower trunk movement in golf

CHRISTOPHER JOYCE[1], ANGUS BURNETT[1,2], & KEVIN BALL[3]

[1]*School of Exercise, Biomedical and Health Sciences, Edith Cowan University, Perth, Australia,* [2]*Department of Sports Science and Physical Education, Chinese University of Hong Kong, Shatin, Hong Kong, and* [3]*School of Sport and Exercise Science, Institute of Sport, Exercise and Active Living, Victoria University, Melbourne, Australia*

(*Received 9 March 2010; revised 4 August 2010; accepted 15 August 2010*)

Abstract
It is believed that increasing the X-factor (movement of the shoulders relative to the hips) during the golf swing can increase ball velocity at impact. Increasing the X-factor may also increase the risk of low back pain. The aim of this study was to provide recommendations for the three-dimensional (3D) measurement of the X-factor and lower trunk movement during the golf swing. This three-part validation study involved; (1) developing and validating models and related algorithms (2) comparing 3D data obtained during static positions representative of the golf swing to visual estimates and (3) comparing 3D data obtained during dynamic golf swings to images gained from high-speed video. Of particular interest were issues related to sequence dependency. After models and algorithms were validated, results from parts two and three of the study supported the conclusion that a lateral bending/flexion-extension/axial rotation (ZYX) order of rotation was deemed to be the most suitable Cardanic sequence to use in the assessment of the X-factor and lower trunk movement in the golf swing. The findings of this study have relevance for further research examining the X-factor its relationship to club head speed and lower trunk movement and low back pain in golf.

Keywords: *Golf, X-factor, lumbar, summation, methods*

Introduction

While the golf ball can be hit with a variety of woods and irons, every golf shot off the tee or the fairway involves a backswing phase and a downswing phase. At the completion of the backswing, the body and the club are positioned in an optimal posture to accelerate the club through the downswing (Hume, Keogh, and Reid, 2005; Hellstrom, 2009). During the downswing, a number of the body's segments are sequenced together to maximise ball velocity at impact (Bechler, Jobe, Pink, Perry, and Ruwe, 1995; Zheng, Barrentine, Fleisig, and Andrews, 2008). The biomechanical principle underlying this motion is termed "summation of velocity" and this is evident for a number of striking/throwing activities such as the tennis serve and baseball pitching (Putnam, 1993).

During the backswing, the shoulders of the golfer are rotated further away from the target than the hips (Myers et al., 2008). The resulting separation of the hip-shoulder alignment at the top of the downswing is referred to as the "X-factor" (McLean, 1992; McTeigue, 1994; Hume et al.,

Correspondence: Christopher Joyce, School of Exercise, Biomedical and Health Sciences Edith Cowan University, 100 Joondalup Drive, Joondalup, Perth, 6027 Australia. E-mail: c.joyce@ecu.edu.au

ISSN 1476-3141 print/ISSN 1752-6116 online © 2010 Taylor & Francis
DOI: 10.1080/14763141.2010.516446

2005; Gluck, Bendo, and Spivak, 2007). Another related concept called the "X-factor stretch" refers to the point after the top of the downswing where the hip-shoulder separation angle is maximised as the hips are known to counter-rotate prior to the shoulders (Cheetham, Martin, and Mottram, 2001). Maximising the hip-shoulder separation angle may increase the potential to utilise the stretch shortening cycle during the golf swing and this has possible implications for increasing hitting distance (Cheetham et al., 2001; Myers et al., 2008). However, a marked hip-shoulder separation angle also has the potential to elevate the risk of developing, or exacerbating low back pain by producing excessive strain on the passive structures of the spine such as the inter-vertebral disc and the facet joints (Lindsay, Horton, and Paley, 2002; Gluck et al., 2007). Therefore, the pathomechanics of low back injury in golfers has also been previously investigated in 3D (Morgan, Cook, Banks, Suagaya, and Moriya, 1998; Lindsay et al., 2002).

There have been various biomechanical approaches utilised when investigating the X-factor (Hellstrom, 2009). Previous researchers have collected three-dimensional (3D) coordinate data and projected the hip-shoulder separation angle (defined as the angle between a line joining the two hip joints and a line joining the two shoulder joints) onto the transverse plane (Myers et al., 2008; Zheng et al., 2008). However, the golf swing is a complex 3D movement with the torso being axially rotated, laterally bent and flexed during the golf swing (Hellstrom, 2009). To this end, the X-factor was recently been reported in a true 3D manner (Horan, Evans, Morris, and Kavanagh, 2010). However, with regards to quantification of 3D rotations, previous studies have been yet to examine multiple body segments (i.e., comparison of shoulders to pelvis, and lower thoracic to pelvis). In previous golf research Wheat, Vernon, and Milner (2007) utilised a multi-segment model projected onto the transverse plane of the trunk (shoulders and thorax). Further, multi-segment models have been used in cricket to investigate lumbar segment kinetics (Ferdinands, Kersting, and Marshall, 2009). Hence, development of a three-segment model for examination of the golf swing is of importance.

When relative rotations of body segments in 3D are described, a concept called "sequence dependency" needs to be considered (Rundquist and Ludewig, 2004; Senk and Cheze, 2006). When defining the position of a rigid body in space, three translations (displacements along the X, Y and Z axes) and three independent and successive rotations (rotation about the X, Y and Z axes – referred to as Cardan angles) are commonly used in Biomechanics (Wu et al., 2002, 2005). In human movement applications these three rotations typically correspond to flexion/extension, lateral bending and axial rotation. To provide anatomical meaning these angles need to be defined in a specific order of rotation (ZYX, ZXY, YZX, YXZ, XYZ or XZY). It is the order in which these angles are defined which may affect the actual value of the rotations reported. While previous authors (Wheat et al., 2007; Horan et al., 2010) have stated the order of rotations utilised when reporting 3D trunk kinematics data during the golf swing the reason for using their Cardanic sequences were not provided. This is of importance as for movements with large magnitudes of rotations about each orthopaedic axis (such as golf), as the magnitude of rotation reported for each Cardanic sequence may vary considerably as the choice of which rotational sequence is appropriate for a particular movement pattern. Lees, Barton, and Robinson (2010) identified a Cardanic sequence of XYZ when analysing the hip and leg movements of the in-step (support) leg of the soccer kick. When compared to the other five Cardanic sequences, the XYZ sequence showed least root mean square values for both orientation angles and angular velocity of the hip and leg segments.

Therefore, the aim of this study was to identify the most appropriate method of examining the X-factor and lower trunk movement in the golf swing via a 3D approach. This was undertaken using a three-segment model and examining the X-factor (shoulders relative to the pelvis) and the magnitude of lower trunk movement (lower thorax relative to the pelvis) and these estimates were compared to visual estimates to ensure anatomical meaningfulness.

Methods

Experimental protocol

The experimental protocol used in this study consisted of three parts: (1) algorithm and model development and validation using a wooden model (2) a comparison of visual estimates of 3D trunk posture and the six Cardanic orders of rotation during representative moments of the golf swing and (3) examination of sequence dependency in real golf swings. To undertake the first part of this study, two motion analysis systems were used as described below. This study was undertaken indoors in the Biomechanics Laboratory at the School of Exercise, Biomedical and Health Sciences, Edith Cowan University. Permission to undertake this research was granted by the Institutional Human Research Ethics Committee.

Data collection

Description of motion analysis systems. Two motion analysis systems were used in this study; an optoelectronic motion analysis system and an electromagnetic tracking system. The optoelectronic system used was a 10-camera MX-F20 Vicon-Peak Motion Analysis system (Oxford Metrics, Oxford, UK) operating at 250 Hz. The electromagnetic tracking system was a 3-Space Fastrak^{TM} (Polhemus Navigation Science Division, Vermont, United States). While the Vicon system was primarily used to define the position and orientation of the segments of interest in this study (pelvis, lower thorax and shoulders) the 3-Space Fastrak^{TM} was used as a "gold standard" in part one of the study (the wooden model trials). The Fastrak has a reported angular accuracy of 0.2° (Pearcy and Hindle, 1989) and this was considered to be slightly better than the 0.6°–1.5° accuracy that angles can be determined with use of the optoelectronic system (Richards, 1999; Elliott Alderson, and Denver, 2007).

The 3-Space Fastrak^{TM} consists of a systems electronics unit, a source and four sensors. The source emits a low-frequency magnetic field that the sensors use to detect their relative three-dimensional (3D) position and orientation. Angular displacement data from the three Fastrak sensors used in this study were output in a ZYX order of rotation at a sampling rate of 30 Hz. With this system positive Z axis points forward, positive Y points right and positive X points up.

Part one – Algorithm and model development and validation. Each of the coordinate systems for the pelvis, lower trunk and shoulders were mimicked on a life-size wooden model in the first part of this study (Figure 1). Representative markers for these coordinate systems were also attached to a human participant during parts two and three of the study. The location of these markers and markers placed on the golf club (used in parts two and three) are shown in Table I. The wooden model was constructed so that flexion/extension and/or lateral bending could be created by purposely bending the flexible wooden rod which simulated the spine (Figure 1). Furthermore, axial rotation could be created in each of the anatomical regions. Consequently, true 3D movement could be created using this model. For the wooden model trials, sensors from the Fastrak system were attached to the simulated "spinous processes" of the three anatomical regions (pelvis, lower trunk and shoulders) (Figure 1b). As each of the simulated pelvis, lower trunk and shoulders on the wooden model were effectively rigid bodies, relative movement measured by the Fastrak was equivalent to that measured by the Vicon system.

After volume calibration for the Vicon system, a series of uni-axial and multi-axial rotation trials were conducted where "shoulders" of the wooden model were moved relative to its "pelvis." During these trials, synchronised kinematic data from the two motion analysis systems were collected. Synchronisation of the Fastrak and Vicon systems was achieved by sending a voltage signal generated from triggering the Fastrak's customised data collection program, to the

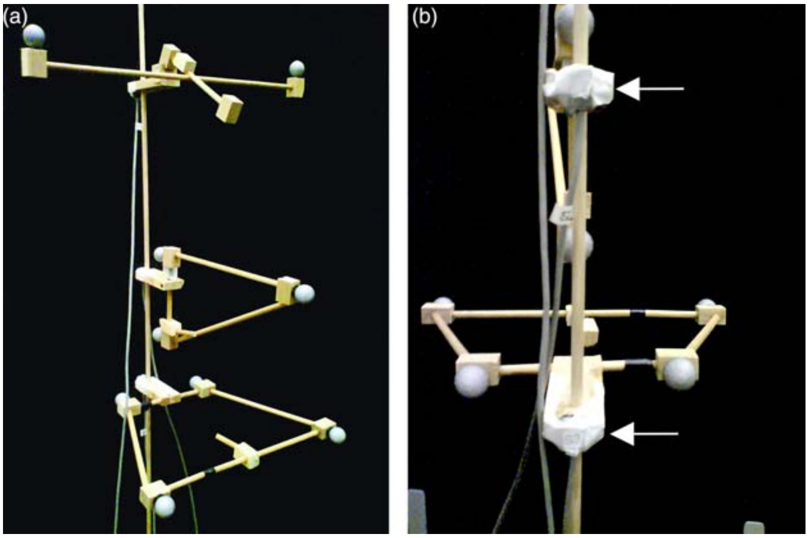

Figure 1. Wooden model used for the validation in part one of the study, Figure shows (a) model with Vicon markers attached and (b) an example of a Fastrak sensor attached to the simulated "spinous processes."

Vicon's Ultranet unit. The trials for this part of the study included; uni-axial rotations (flexion, extension, left and right lateral flexion, left and right axial rotation) and a multi-axial rotation (a simulated golf back-swing trial). While the design of the wooden rod could not completely eliminate the coupling of rotation during the single-axis trials, they were conducted so that a vast majority of rotation occurred about the axis of interest. In each of these trials, data were collected for approximately 5–8 seconds. Data from these trials were smoothed using a Woltring filter with a mean square error of 20. All data from these trials were then exported to text files for further analysis.

Table I. Anatomical placements of light-reflective Vicon markers.

Markers	Anatomical marker placement
Shoulder ref. frame	
Left shoulder	Left acromion process
Right shoulder	Right acromion process
Lower thorax ref. frame	
Sternum	Xiphoid process, distal end of the sternum
T10 vertebrae	Tenth thoracic spinous process (T10)
L1 vertebrae	First lumbar spinous process (L1)
Pelvis ref. frame	
Left anterior pelvis	Left anterior superior illiac spine (LASIS)
Right anterior pelvis	Right anterior superior illiac spine (RASIS)
Left posterior pelvis	Left posterior superior illiac spine (LPSIS)
Right posterior pelvis	Right posterior superior illiac spine (RPSIS)
Golf club ref. frame	
Upper shaft	1/3 length of shaft from grip
Lower shaft	2/3 length of shaft from grip

Part two – Visual estimations of 3D posture. A comparison of visual estimates of 3D trunk posture and the six Cardanic orders of rotation was conducted at five distinct moments of the golf swing (address, take-away, top of backswing, impact and follow-through). The purpose of this part of the study was to conduct a "face-validity" type analysis prior to conducting dynamic analysis of the golf swing. Visual estimates of range of motion (in 2D) is routinely used in clinical practice and in previous research investigating shoulder pain (Terwee et al., 2005) and passive range of motion in the lower limbs of children (Rachkidi et al., 2009).

In the current study a single examiner (an experienced Sports and Clinical Biomechanist with knowledge of the relevant mathematical procedures) estimated the 3D trunk posture of a male subject who was asked to assume the five static positions. These postures were assessed as being representative of the golf swing by the Head Teaching Professional from a private golf club with over seven years of golf coaching and swing analysis. For each of the five static positions, the visual examiner was asked to report the 3D trunk posture (flexion/extension, lateral bending and rotation) for the shoulders relative to the pelvis and the lower trunk relative to the pelvis to the nearest 5° (Terwee et al., 2005; Rachkidi et al., 2009).

Vicon data were collected while the subject was in an anatomical position, and for each of the five static positions. Once the static position was set and the Vicon data were collected, the examiner was able to move around the subject to estimate their 3D trunk posture. This process was repeated for each of the five static positions. Three observers watched this process and agreed the subject displayed minimal movement while being observed. The analysis of the visual estimates and the Vicon data was conducted in a blinded manner.

Part three – Golf swing trials. Dynamic golf swing trials were carried out with the Vicon system using a single participant. The participant for this part of the study was a male golfer who played with a seven handicap. Retro-reflective markers were attached to the golfer and for the purpose of identifying the top of the backswing; two markers were also added to the golf club (Table I). Furthermore to identify impact, a small piece of retro-reflective tape was attached to the golf ball. After a suitable warm-up and volume calibration, the participant was then filmed performing six range of motion trials (same single –plane movements as in part one of the study). A trial was also captured with the participant standing in an anatomical position so that movements during the golf swing could be measured relative to the neutral position. The participant then hit a total of 10 maximal effort shots using a leading brand driver and a five-iron. These clubs were used as they are representative of the two types of clubs (i.e., a driver and an iron) used in golf (Wells, Elmi, and Thomas, 2009). All shots involved hitting the same leading brand of golf ball off an artificial turf surface into a net placed positioned 5 m in front of the hitting area. From the 10 golf swings recorded, two trials (one for the driver, one for the five-iron) were chosen for analysis based on maximal club-head velocity and minimal marker loss. No variables pertaining to hitting accuracy were quantified in this study.

In this phase of testing, the golf swing trials were also recorded using two Sony HDRFX7 (HD1080i) high-speed video cameras operating at a 300 Hz with a shutter speed of 1/3000 s. These cameras were positioned perpendicular to the hitting area and from behind the participant. The footage from these cameras was used to visually confirm which order of rotation provided the closest estimate of what was happening anatomically. The Vicon system and high-speed cameras were synchronised using impact as the critical event. Vicon data from these trials were smoothed using a Woltring filter with a mean square error of 20 and the resulting data were then exported as a text file.

Table II. Joint coordinate systems (JCS) for shoulder, lower thorax and pelvis.

JCS	Origin	X – vector	Y (temp) – vector	Z – vector	Y – vector
Shoulder					
	Coincident with the mid-acromion and halfway to T10	Mid-acromion point, with the unit vector pointing to the right	Mid-point of the mid-acromion and T10, a distal unit vector, perpendicular to X	The common perpendicular of X and Y (temp), a proximal unit vector, perpendicular to X	Cross-product of X and Z, unit vector perpendicular and anterior to X
Lower thorax					
	Coincident with the mid-point of L1 and T10 and halfway to Sternum	Mid-point of L1 and T10, with the unit vector pointing to the right	Mid-point of the L1 and Sternum, a distal unit vector, perpendicular to X	The common perpendicular of X and Y (temp), a proximal unit vector, perpendicular to X	Cross-product of X and Z, unit vector perpendicular and anterior to X
Pelvis					
	Coincident with the mid-point of mid-ASIS and mid-PSIS	Mid-point of mid-ASIS and mid-PSIS, unit vector pointing to the right	Mid-point of the mid-ASIS and mid-PSIS, a distal unit vector, perpendicular to X	The common perpendicular of X and Y (temp), a proximal unit vector, perpendicular to X	Cross-product of X and Z, unit vector perpendicular and anterior to X

Data analysis – Algorithm and model development and validation

Part one – Fastrak data. Relative rotations (flexion/extension, lateral bending and axial rotation) in each of the six Cardanic orders of rotation were determined for the shoulders relative to the pelvis (X-factor) and the lower thorax relative to the pelvis (lower trunk angle). To calculate these variables, the following process was undertaken.

First, the three Cardan angles for each sensor (relative to the source) were used to determine the direction cosine matrix for each sensor. Second; the transposed direction cosine matrix of the proximal sensor and the direction cosine matrix of the distal sensor were multiplied and the relative rotations (still in ZYX order) were recovered. Finally; in order to calculate the rotations relative to a zero reference (0, 0, 0) the direction cosine matrix from where the Cardan angles were reduced was multiplied by the direction cosine matrix derived from the first frame of data from each trial (Burnett, Barrett, Marshall, Elliott, and Day, 1998). Fastrak data captured at 30 Hz were time-matched to Vicon data recorded at 250 Hz using cubic spline interpolation.

Part one – Vicon data. Smoothed coordinate data from the retro-reflective markers were used to construct the joint coordinate systems (JCS) (Grood and Suntay, 1983; Wren and Mitiguy, 2007). To be consistent with the coordinate system of the Fastrak the same axes definition was used for the Vicon data. These were defined as outlined below.

After these JCS were constructed, the Cardan angles related to the shoulders relative to the pelvis (X-factor) and the lower thorax relative to the pelvis (lower trunk movement) were calculated by the same means as the Cardan angles reduced from the Fastrak.

Part two – Visual estimations of 3D posture. To examine the effect of sequence dependency during the static posture trials, the three angles were calculated for the six Cardanic orders of rotation. The results from the visual examination of trunk posture; flexion/extension (Y), lateral bending (Z) and axial rotation (X) for each of the five static trials were compared against each order of rotation (ZYX, ZXY, YXZ, YZX, XZY and XYZ), reduced as outlined above.

Part three – Golf swing trials. To examine the effect of sequence dependency on dynamic golf swing trials, the Y, Z and X values were calculated for the six Cardanic orders of rotation. These values were calculated at the top of the backswing and at impact. The top of the backswing was determined as the frame in which the transition point from backswing to downswing was made (Myers et al., 2008). From the Vicon algorithm, the maximal value of axial rotation in the back swing was also consistent with the transition point or frame, which could be seen. Impact was defined as the frame where the ball was first seen to move after contact. The identification of the top of the backswing in the high-speed video footage was determined by time matching back from the moment of impact as determined by the Vicon system. This and all previous analyses were undertaken using Microsoft Excel.

Statistical analysis

In part one of the study, to determine the similarity between Fastrak and Vicon kinematic data for the six uni-axial trials and the multi-axial trial, two indices were used; the adjusted coefficient of multiple correlation (CMC), R_a^z, (Kadaba et al., 1989) and the Mean Absolute Variability (MAV) (e.g., Noonan et al., 2003). CMC values of 1 indicate identical waveforms while lower MAV values (data are in degrees) indicate more similarity between two sets of kinematic data. In part two of the study, comparisons of the visual estimates of trunk posture and the six orders of rotation were quantified by calculating the averaged magnitude of the vector from the three angles for the two methods of analysis. In part three of the study descriptive data from the six Cardanic sequences were presented in combination with images taken from the high-speed footage at transition and impact.

Results

Part one – Algorithm and model development and validation

CMC and MAV values for the six ranges of motion trials and the one multi-axis trial are shown in Table III. The average CMC value obtained for all seven trials was 0.998 which demonstrated a very high level of similarity between the Vicon and Fastrak data. Furthermore, the average MAV value obtained from all seven trials was 0.6°. These results confirmed that the algorithms and models developed in part one of this study were valid.

Part two – Visual estimations of 3D posture

The averaged magnitude of the differences between the visual estimations and the six Cardanic orders of rotation (from Vicon analysis) for the static positions of the golf swing are presented in Table IV. From these data it can be seen that when the shoulder relative to pelvis and the lower thorax relative to pelvis data are summed together, the ZYX (Lateral Bend-Flexion/Extension-Axial Rotation) order of rotation shows the closest agreement between visual estimates and motion analysis derived data. While it would be ideal to conclude from these results that the ZYX sequence most closely approximates what is seen visually, the precision of visual estimates prevented the selection of one sequence from this phase of analysis.

Part three – Golf swing trials

After obtaining angle-time data for the dynamic trials (see samples in Figure 4a and 4b), data related to the X-factor and lower lumbar position at the top of the backswing and impact for the driver and five-iron trials were derived. From these data a great disparity in the flexion-extension, lateral bending and axial rotation angles between the six rotational sequences was evident (Tables V and VI). The process of determining the most appropriate Cardanic sequence to analyse dynamic golf swing trials involved eliminating orders of rotation that did not represent what was seen visually (Figures 2 and 3). As this study was predominantly interested in quantifying rotational (X) values (e.g., X-factor) a closeness in approximation of X values was seen as the most important priority. In the XYZ, XZY and ZXY sequences there were major discrepancies between Vicon data and what was seen in the images obtained from high-speed film for both shoulder – pelvis and lower thorax – pelvis. With these three orders of rotation eliminated, lateral bending (Z) was then assessed from the three remaining Cardanic sequences. On the basis that the YXZ order of rotation showed over-estimated values at the top of the backswing (Tables V and VI) this sequence was then eliminated. From the two remaining orders of rotation (ZYX and YZX), flexion/extension values (Y) were examined and due to the position of the shoulders relative to the pelvis at the top of the backswing (Figures 2 and 3), flexion (negative) values were determined to be more representative rather than extension (positive) values. More representative data are also seen in the driver and five-iron trials at the top of the backswing (Tables Va and VIa), where the longer club (driver) causes lesser values of flexion. Negative flexion values were also seen at impact (Tables Vb and VIb). To further support the

Table III. Comparison of Vicon and Fastrak data.

ROM	Coefficient of multiple correlation (CMC)	Mean absolute variability (°) (MAV)
Trunk flexion	0.999	1.1
Trunk extension	0.997	0.9
Right lateral flexion	0.999	0.1
Left lateral flexion	0.999	0.2
Right axial rotation	0.998	0.2
Left axial rotation	0.998	1.4
Set-up to top of backswing (right axial rotation for golf specific movement pattern)	0.999	0.4
Average scores	**0.998**	**0.6**

Note: Coefficient of multiple correlation (CMC) and mean absolute variance (MAV) statistics.

choice of the ZYX sequence, the YZX sequence also showed relatively small and positive values of rotation (X) for lower thorax – pelvis at the top of the backswing (Figures 2a and b, 3a and b) when there is a clear flexed trunk posture at this point for shoulders – pelvis. Finally, angle-time data for the ZYX order of rotation (Figures 4 and 5) appeared to most closely match what was seen visually.

Discussion

Recently, there has been an increased amount of attention paid to the biomechanics of the golf swing and particularly phenomena such as the X-factor (e.g., Hume et al., 2005; Gluck et al., 2007). However, there are few recommendations on how to report such data in a true 3D manner. It has been previously reported that for small joint rotations, the choice of Cardanic sequence is relatively unimportant (Crawford, Yamaguchi, and Dickman, 1996; McGill, Chloewicki, and Peach, 1997) however, as Cardan angles approach 90°, large coupled rotations appear and the choice of Cardanic sequence becomes more important. (Rundquist and Ludewig, 2004). As the golf swing involves large rotational motion of the trunk, the aim of this study was to investigate methodological considerations for examining the X-factor and lower trunk movement in 3D during the golf swing. Previous biomechanical analyses of movement have rarely justified the choice of a Cardanic sequence for 3D analyses (Leardini et al., 2009).

In this study, the choice of what Cardanic sequence to utilise in 3D biomechanical analysis was undertaken using a multi-step validation procedure. Specifically, after validating the algorithms and model (part one) using a similar approach to that reported in previous research (e.g., Cutti, Geovanardini, Rocchi, Davalli, and Sacchetti, 2008), visual estimation of 3D trunk posture at five critical points during the golf swing (part two), and visual comparison to two critical points during actual golf swings (as taken from high-speed footage in part three) was used as a basis for comparison. From these procedures it was determined that the ZYX order of rotation (corresponding to lateral bending, flexion/extension, axial rotation) seemed the most suitable for analysis of a rotation-dominant movement such as the golf swing.

Some recommendations for the reporting of 3D kinematic data have been previously provided in the literature. First, the International Society of Biomechanics (ISB) (Wu and Cavanagh, 1995; Wu et al., 2002; Wu et al., 2005) suggests that kinematic data should be

Table IV. Averaged visual estimation values of the static 3D trials using magnitude of difference.

	Trial	ZYX	YZX	XYZ	XZY	ZXY	YXZ
Shoulder vs pelvis	Address	13.7	14.6	14.4	24.8	20.6	17.5
	Take away	11.7	9.3	22.1	39.8	28.2	30.2
	Transition	10.8	42.1	51.3	50.5	6.4	49.4
	Impact	14.7	15.9	23.1	32.6	29.4	31.0
	Follow through	17.7	18.5	60.0	48.6	96.8	40.8
	Mean	**13.7**	**20.1**	**34.2**	**39.3**	**36.3**	**33.8**
Lower thorax vs pelvis	Address	6.8	8.6	24.2	8.1	4.7	8.6
	Take away	4.6	12.6	9.9	10.7	13.8	13.7
	Transition	13.7	32.6	29.1	22.7	29.2	29.4
	Impact	7.2	4.8	12.3	5.4	9.7	5.7
	Follow through	15.4	15.6	16.9	15.4	46.3	17.9
	Mean	**9.5**	**14.8**	**18.5**	**12.5**	**20.7**	**15.0**

reported so that angles remain as close as possible to the clinical definitions of joint and segment motions. These guidelines also mention that proximal and distal segments be clearly defined, and that the choice of the centre of origin of the segments can drastically affect angular displacement values (Wu and Cavanagh, 1995). Crawford et al. (1996) utilised both Cardan and projected angles for finding the most representative Cardanic sequence for assessing spine motion. It was stated that while any of the six orders of rotation could be used, for spinal motion of small magnitude the flexion-extension, lateral bending and axial rotation sequence was recommended. The choice of an appropriate order of rotation has previously been reported for movements with large movements of the trunk such as fast bowling in cricket. In this study, a Cardanic sequence of lateral bending, flexion-extension and axial rotation order was recommended (Ferdinands et al., 2009).

Table V. Cardan angles (°) for each of the six rotational sequences for the driver swing.

	ZYX	YZX	XYZ	XZY	ZXY	YXZ
Top of backswing						
Shoulder vs pelvis						
Flexion	−15.0	12.8	−13.2	−23.4	29.7	−2.1
Lat bend	3.8	23.7	−64.2	72.8	−3.3	48.3
Rotation	−71.9	−70.6	−46.7	−17.2	−123.5	−72.3
Lower thorax vs pelvis						
Flexion	−17.7	31.1	157.8	−15.4	−40.0	31.7
Lat bend	19.9	26.9	28.0	22.3	44.8	30.9
Rotation	−42.2	13.1	−13.2	−12.6	23.4	14.0
Ball impact						
Shoulder vs pelvis						
Flexion	−22.5	−27.6	−39.8	1.4	3.2	−49.2
Lat bend	−35.4	−36.3	−40.5	21.7	−65.9	−29.4
Rotation	−17.8	−16.7	−13.0	−35.8	−71.7	7.6
Lower thorax vs pelvis						
Flexion	−0.9	−14.2	131.1	−17.5	−18.5	14.3
Lat bend	−16.1	−13.9	−10.9	−13.2	−16.8	−15.9
Rotation	−18.4	−3.4	−8.1	−3.5	−4.3	−3.6

Note: The angles are consistent with the top of the backswing and ball impact. Positive values indicate right lateral bending, trunk extension and left axial rotation.

Table VI. Cardan angles (°) for each of the six rotational sequences for the five-iron swing.

	ZYX	YZX	XYZ	XZY	ZXY	YXZ
Top of backswing						
Shoulder vs pelvis						
Flexion	− 19.1	1.6	− 9.1	− 39.0	28.0	− 11.8
Lat bend	3.8	18.1	40.9	68.4	− 5.9	− 61.7
Rotation	− 70.3	− 69.3	− 69.4	− 24.3	− 124.5	− 45.3
Lower thorax vs pelvis						
Flexion	− 18.3	27.7	27.9	− 13.0	− 39.5	160.3
Lat bend	19.3	24.8	29.5	21.7	41.4	28.8
Rotation	− 40.4	12.4	13.6	− 11.0	19.6	9.4
Ball impact						
Shoulder vs pelvis						
Flexion	− 32.5	− 37.9	− 48.4	− 11.2	5.7	− 49.6
Lat bend	− 36.3	− 38.0	− 43.9	30.0	− 65.1	− 34.0
Rotation	− 27.4	− 26.0	4.2	− 38.2	− 91.0	− 35.6
Lower thorax vs pelvis						
Flexion	− 7.8	11.8	12.0	− 16.0	− 28.3	151.5
Lat bend	− 12.7	− 10.1	− 9.8	− 7.9	− 11.7	− 12.6
Rotation	− 22.7	− 3.2	− 2.8	− 3.0	3.9	1.8

Note: The angles are consistent with the top of the backswing and ball impact. Positive values indicate right lateral bending, trunk extension and left axial rotation.

The findings of this study provide evidence that some previous recommendations should be adopted with caution. For instance, McGill et al. (1997) stated that the axis first experiencing 90°of rotation should be defined first in a sequence of three rotations so that errors in the other two axes are minimised. With axial rotation being the largest value of rotation in golf (Figures 3 and 4) this would mean that either of the XYZ or XZYorders of rotation could be chosen. From the data reported in this study, this would have created data sets that do not describe what is seen visually. Wheat et al. (2007) using a dual-segment model, used the Cardan sequence YZX for determining hip-shoulder rotations, which does not support McGill's recommendations. Lees et al. (2010) suggested the largest movement of the soccer kick was flexion-extension of the hip (Y), which also does not support McGill's recommendations, as they recommended either the XYZ or XZYas the *de facto* standard through analysis of the six Cardanic sequences, and also the support of multiple references.

A limitation of this study was that a face-validity process was utilised. That is, the angles reported needed to be consistent with what was visualised. A more precise gold standard may have been achieved by using a goniometer. An example of such an approach would be the mechanical arm study of Elliott et al. (2007). However, with the reporting of estimated angles in increments of 5° in part two of this study (Terwee et al., 2005; Rachkidi et al., 2009) there were sufficiently large differences evident between Cardanic sequences to enable the elimination of certain sequences of rotation.

A second limitation was that the 2D method in which the X-Factor has been previously reported (McLean, 1992; Myers et al., 2008) which requires a vector to be created through the left and right acromion processes. However, for 3D analysis of X-factor in this study, the shoulder coordinate system was constructed from both acromion landmarks and T10. There are some difficulties with such a representation of shoulder alignment. For example, movement of the landmarks used in the reconstruction of shoulder alignment, such as scapula retraction, can lead to large calculation errors (Elliott, Wallis, Sakurai, Lloyd, and Besier, 2002). However,

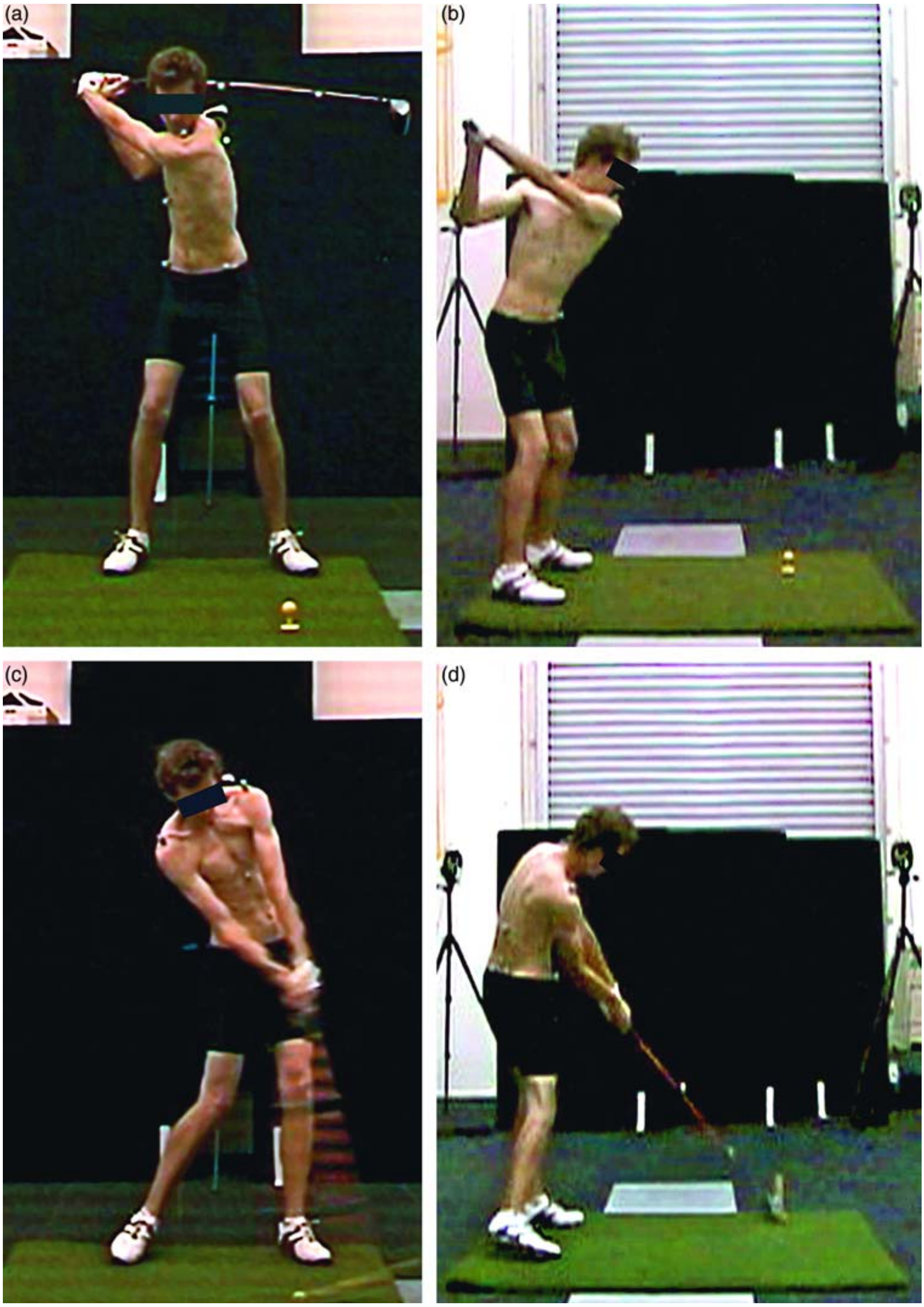

Figure 2. Frames from the high-speed footage for the (a) sagittal view for the top of the backswing (b) rear view for the top of the backswing (c) sagittal view at impact and (d) rear view at impact for a selected driver trial.

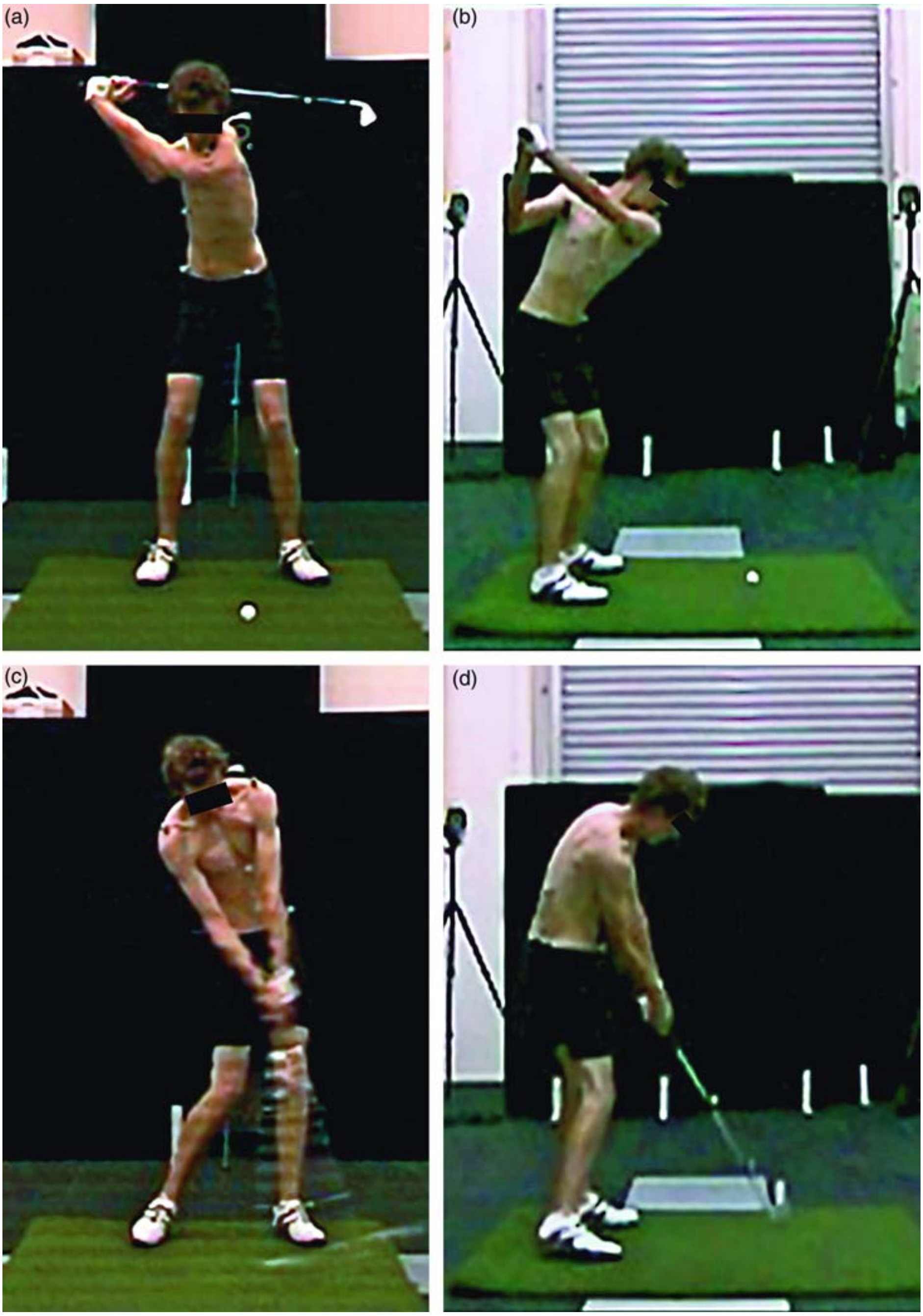

Figure 3. Frames from the high-speed footage for the (a) sagittal view for the top of the backswing (b) rear view for the top of the backswing (c) sagittal view at impact and (d) rear view at impact for a selected five-iron trial.

this representation of the shoulder alignment typifies the concept of the X-factor and 2D projection of shoulder alignment in certain phases of the fast bowling motion is still used (Elliott et al., 2002). Results from the two studies that used transverse projected angles showed

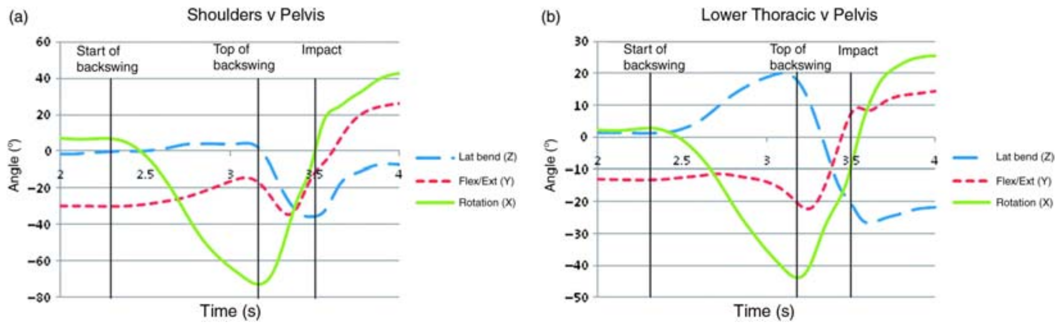

Figure 4. Angle-time data for the dynamic golf swing trials in Part 3 of testing. Shown are the angles from the ZYX Cardanic sequence for the (a) Shoulder vs Pelvis and (b) Lower Trunk vs Pelvis.

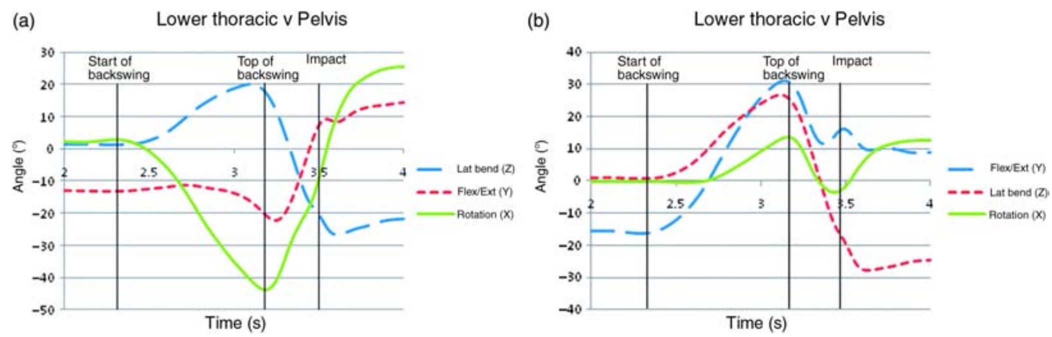

Figure 5. Angle-time data for the dynamic golf swing trials in Part 3 of testing. Shown are the angles from the (a) ZYX and (b) YZX Cardanic sequences for the Lower Thoracic vs Pelvis to determine the most accurate order of rotation.

a projected X-factor of 61.8° ± 7.8° (Myers et al., 2008) and 55° ± 10° (Zheng et al., 2008) for high-velocity swings. These values were consistent with what was found in this study for the Cardanic sequence ZYX (Tables V and VI).

Calculation errors due to shoulder alignment may also influence the choice of Cardanic sequence. Wheat et al. (2007) used the YZX order of rotation as the most appropriate, although the thoracic segment was made up of five individual markers, whereas the shoulder segment used in this study was made up of only three. The fact that the closeness of the ZYX and the YZX Cardanic sequences seen in this study suggest that the choice of markers, number of markers used to construct a segment and the number of segments may influence the Cardanic sequence used. Lees et al. (2010) suggested that either the XYZ or the XZY sequence support dynamic leg movements in soccer, although multiple studies had suggested the XYZ sequence to be the *de facto* standard. With this in mind, more studies are needed to support the choice Cardanic sequence for the golf swing.

While this study is a methodological investigation, it is of importance to both practitioners and coaches as it provides the methodological basis for examining issues related to analysing the golf swing such as the summation of segments. The results shown from this study have further strengthened the use of multi-segment models due to the kinematics of the trunk during the golf swing, and the potential for its use alongside X-factor-type analyses.

Acknowledgements

The authors wish to thank the Western Australian Institute of Sport for lending the authors the high-speed video camera and golf teaching professional Mr Nic D'Avoine for his assistance with part two of the study.

References

Bechler, J. R., Jobe, F. W., Pink, M., Perry, J., and Ruwe, P. A. (1995). Electromyographic analysis of the hip and knee during the golf swing. *Clinical Journal of Sports Medicine*, *5*, 162–166.

Burnett, A. F., Barrett, C. J., Marshall, R. N., Elliott, B. C., and Day, R. E. (1998). Three-dimensional measurement of lumbar spine kinematics for fast bowlers in cricket. *Clinical Biomechanics*, *13*, 574–583.

Cheetham, P., Martin, P., and Mottram, R. (1994). The importance of stretching the "X-factor" in the downswing of golf: The "X-factor stretch". In P. R. Thomas (4th ed., Ed.), *Optimising performance in golf* (pp. 192–199). Brisbane (QLD): Australian Academic Press.

Crawford, N. R., Yamaguchi, G. T., and Dickman, C. A. (1996). Methods of determining spinal flexion/extension, lateral bending, and axial rotation from marker coordinate data: Analysis and refinement. *Human Movement Science*, *15*, 55–78.

Cutti, A. G., Geovanardini, A., Rocchi, L., Davalli, A., and Sacchetti, R. (2008). Ambulatory measurement of shoulder and elbow kinematics through inertial and magnetic sensors. *Medical and Biological Engineering and Computing*, *46*, 169–178.

Elliott, B. C., Alderson, J. A., and Denver, E. (2007). System and modelling errors in motion analysis: Implications for the measurement of the elbow angle in cricket bowling. *Journal of Biomechanics*, *40*, 2679–2685.

Elliott, B. C., Wallis, R., Sakurai, S., Lloyd, D., and Besier, T. (2002). The measurement of shoulder alignment in cricket fast bowling. *Journal of Sport Sciences*, *20*, 507–510.

Ferdinands, R. E. D., Kersting, U., and Marshall, R. N. (2009). Three-dimensional lumbar segment kinetics of fast bowling in cricket. *Journal of Biomechanics*, *42*, 1616–1621.

Gluck, G. S., Bendo, J. A., and Spivak, J. M. (2007). The lumbar spine and low back pain in golf: A literature review of swing biomechanics and injury prevention. *The Spine Journal*, *7*, 1–11.

Grood, E. S., and Suntay, W. J. (1983). A joint coordinate system for the clinical description of three-dimensional motions: Application to the knee. *Journal of Biomechanical Engineering*, *105*, 136–144.

Hellstrom, J. (2009). Competitive elite golf: A review of the relationships between playing results, technique and physique. *Sports Medicine*, *39*, 723–741.

Horan, S. A., Evans, K., Morris, M. R., and Kavanagh, J. J. (2010). Thorax and pelvis kinematics during the downswing of male and female skilled golfers. *Journal of Biomechanics*, *43*, 1456–1462.

Hume, P. A., Keogh, J., and Reid, D. (2005). The role of biomechanics in maximising distance and accuracy of golf shots. *Sports Medicine*, *35*, 429–449.

Kadaba, P., Ramakrishnan, H. K., Wootten, M. E., Gainey, J., Gorton, G., and Cochran, G. V. B. (1989). Repeatability of kinematic, kinetic and electromyographic data in normal adult gait. *Journal of Orthopaedic Research*, *7*, 849–860.

Leardini, A., Biagi, F., Belvedere, C., and Benedetti, M. G. (2009). Quantitative comparison of current models for trunk motion in human movement analysis. *Clinical Biomechanics*, *24*, 542–550.

Lees, A., Barton, G., and Robinson, M. (2010). The influence of cardan rotation sequence on angular orientation data for the lower limb in the soccer kick. *Journal of Sport Sciences*, *28*, 445–450.

Lindsay, D. M., Horton, J. F., and Paley, R. D. (2002). Trunk motion of male professional golfers using two different golf clubs. *Journal of Applied Biomechanics*, *18*, 366–373.

McGill, S. M., Chloewicki, J., and Peach, J. P. (1997). Methodological considerations for using inductive sensors (3space isotrak) to monitor 3D orthopaedic joint motion. *Clinical Biomechanics*, *12*, 190–194.

McLean, J. (1992). Widen the gap. *Golf Magazine*, *12*, 49–53.

McTeigue, M., Lamb, S. R., and Mottram, R. (1994). Spine and hip motion analysis during the golf swing. In A. J. Cochran, and M. R. Farrally (Eds.), *Science and golf II: Proceedings of the World Scientific Congress of Golf* (pp. 50–58). London: E & FN Spon.

Morgan, D., Cook, F., Banks, S., Suagaya, H., and Moriya, H. (1998). The influence of age on lumbar mechanics during the golf swing. In A. J. Cochran, and M. R. Farrally (Eds.), *Science and golf III: Proceedings of the World Scientific Congress on Golf* (pp. 120–126). Champaign, IL: Human Kinetics.

Myers, J., Lephart, S., Tsai, Y. S., Sell, T., Smoliga, J., and Jolly, J. (2008). The role of upper torso and pelvis rotation in driving performance during the golf swing. *Journal of Sport Sciences*, *26*, 181–188.

Noonan, K. J., Halliday, M. S., Browne, R., O'Brien, S., Kayes, K., and Feinberg, J. (2003). Inter-observer variability of gait analysis with cerebral palsy. *Journal of Paediatric Orthopaedics*, *23*, 279–287.

Pearcy, M. J., and Hindle, R. J. (1989). Rotational mobility of the human back in forward flexion. *Journal of Biomechanical Engineering*, *11*, 219–223.

Putnam, C. A. (1993). Sequential motions of body segments in striking and throwing skills: Descriptions and explanations. *Journal of Biomechanics*, *26*, 125–135.

Rachkidi, R., Ghanem, I., Kalouche, I., El Hage, S., Dagher, F., and Kharrat, K. (2009). Is visual estimation of passive range of motion in the paediatric lower limb valid and reliable. *BMC Musculoskeletal Disorders*, *10*, 126–136.

Richards, J. G. (1999). The measurement of human motion: A comparison of commercially available systems. *Human Movement Science*, *18*, 589–602.

Rundquist, P. J., and Ludewig, P. M. (2004). Patterns of motion loss in subjects with idiopathic loss of shoulder range of motion. *Clinical Biomechanics*, *19*, 810–818.

Senk, M., and Cheze, L. (2006). Rotation sequence as an important factor in shoulder kinematics. *Clinical Biomechanics*, *21*, S3–S8.

Terwee, C. B., de Winter, A. F., Scholten, R. J., Jans, M. P., Deville, W., van Schaardenburg, D., et al. (2005). Interobserver reproducibility of the visual estimation of range of motion of the shoulder. *Archives of Physical Medicine & Rehabilitation*, *86*, 1356–1361.

Wells, G. D., Elmi, M., and Thomas, S. (2009). Physiological correlates of golf. *Journal of Strength and Conditioning Research*, *23*, 741–750.

Wheat, J. S., Vernon, T., and Milner, C. E. (2007). The measurement of upper body alignment during the golf drive. *Journal of Sports Sciences*, *25*, 749–755.

Wren, T. A. L., and Mitiguy, P. C. (2007). A simple method to obtain consistent clinically meaningful pelvic angles from euler angles during gait analysis. *Journal of Applied Biomechanics*, *23*, 218–223.

Wu, G., and Cavanagh, P. R. (1995). ISB recommendations for standardisation in the reporting of kinematic data. *Journal of Biomechanics*, *28*, 1257–1261.

Wu, G., Siegler, S., Allard, P., Kirtley, C., Leardini, A., Rosenbaum, D., et al. (2002). ISB recommendation on definitions of joint coordinate system of various joints for the reporting of human joint motion – part I: Ankle, hip and spine. *Journal of Biomechanics*, *35*, 543–548.

Wu, G., van der Helm, F. C. T., Veeger, H. E. J., Makhsous, M., Van Roy, P., Anglin, C., Nagels, J., et al. (2005). ISB recommendation on definitions of joint coordination systems of various joints for the reporting of human joint motion – Part II: shoulder, elbow, wrist and hand. *Journal of Biomechanics*, *38*, 981–992.

Zheng, N., Barrentine, S. W., Fleisig, G. S., and Andrews, J. R. (2008). Kinematic analysis of the swing in pro and amateur golfers. *International Journal of Sports Medicine*, *29*, 487–493.